ACS APPLIED MATERIALS & INTERFACES

Forum Article

www.acsami.org

A General Strategy to Create RNA Aptamer Sensors Using "Regulated" Graphene Oxide Adsorption

Jinping Song,[†,‡,§,⊥] Pui Sai Lau,[†,⊥] Meng Liu,[†] Shaomin Shuang,[‡] Chuan Dong,*[,‡] and Yingfu Li*[,†]

[†]Department of Biochemistry and Biomedical Sciences, Department of Chemistry and Chemical Biology, McMaster University, 1280 Main Street West, Hamilton, Ontario L8S 4M1, Canada

[‡]Institute of Environmental Science, Shanxi University, Taiyuan 030006, China

Supporting Information

ABSTRACT: Aptamers have been used as molecular recognition elements for sensor development in combination with graphene oxide (GO), a nanomaterial with properties including fluorescence quenching, and selective adsorption of single-stranded nucleic acids. However, previous sensor designs based on aptamer-GO adsorption have not demonstrated wide applicability, and few studies have explored the potential of RNA aptamers. Herein, we present a new sensing strategy based on "regulated" GO adsorption that can accommodate various RNA aptamers. First, adsorption of a fluorophore-labeled RNA aptamer to GO results in fluorescence quenching due to close proximity of the fluorophore to GO. The addition of a complementary, "blocking" DNA strand (BDNA) that hybridizes to the 3′-end of the aptamer, weakens aptamer-GO interaction, and enables increased fluorescent signal generation upon the addition of target, as the sensing system becomes completely separated from GO. Our findings can be applied toward different aptamers, and adapted to enhance generality of existing sensing applications.

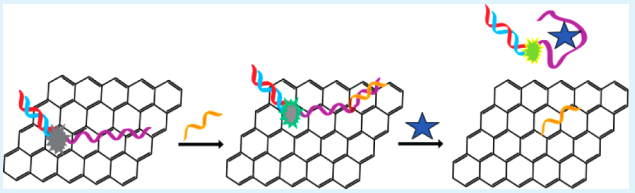

KEYWORDS: *aptamers, RNA, sensors, graphene oxide, fluorescence*

1. INTRODUCTION

Design generality provides a set of guiding principles that can be applied to create diverse systems for various applications. Hence, effective design generality can extend applicability beyond initial proof-of-concept demonstration, to also greatly facilitate future advancement of a field, which is especially important for emerging technologies.

A notable emerging nanomaterial is graphene.[1] Made up of a single-layer lattice of hexagonal carbon, graphene possesses many useful properties including high surface area, mechanical strength, conductivity, biocompatibility, fluorescence quenching ability, and amenability to functionalization.[2−7] Since its discovery in 2004,[1] graphene has made tremendous contributions toward various applications largely because of well-established generalizable strategies. For example, efficient, environmentally safe and cost-effective chemical methods have been developed to synthesize graphene in large scale[8−12] facilitating industrial application and commercialization.[13,14] Furthermore, general strategies to engineer graphene-based devices are on the rise, enabling higher performance of airplanes and automobiles, energy generating and storage devices, as well as medical implants.[14,15] Additionally, methods are also becoming well-established to implement graphene materials as a potential platform to transport therapeutic agents into cancer cells for treatment.[16−19]

Though still relatively early in progress, graphene and its derivatives have also made considerable advancements for sensor development, particularly implementing aptamers as molecular recognition elements.[5,20−26] Aptamers are single-stranded DNA or RNA molecules that fold into a defined tertiary structure to bind a designated target.[27,28] These unique molecular probes have been widely implemented for fluorescence-based detection due to ease in aptamer labeling, and availability of detection instruments.[29,30]

In several reported studies, the oxidized form of graphene, graphene oxide (GO) has been applied as a fluorescence quencher in fluorescence resonance energy transfer (FRET)-based detection using aptamers.[5,20−26] Typically, these designs make use of the ability of GO to preferentially bind the aptamer in its free, single-stranded state rather than the state where the aptamer is target-bound. Hence, adsorption of a fluorescently labeled aptamer to GO, results in fluorescence quenching through FRET. The addition of target, however, results in conformational change or "structure-switching"[31,32] of the aptamer to form the aptamer-target complex. The subsequent disruption of FRET generates a high fluorescent signal.

This strategy of GO functionalization through noncovalent adsorption of the aptamer possesses many advantages compared to covalent strategies including the preservation of intrinsic GO properties, and the simplicity of functionalization

Special Issue: Materials for Theranostics

Received: April 9, 2014
Accepted: June 24, 2014
Published: July 3, 2014

without the need of any coupling reagents.[33] However, this strategy may not be generally applicable to many aptamers, particularly longer sequences. The binding interaction of single-stranded nucleic acids to GO typically becomes greater with increasing sequence length,[34−36] and adsorption strength is also a function of nucleotide composition.[37] For these reasons, the relatively stronger GO adsorption from longer aptamers or aptamers composed of stronger-binding nucleotides is likely to out-compete the formation of target-aptamer complex, especially when dealing with low-affinity aptamers. Although previously reported studies have successfully implemented this strategy for sensing, it must be noted that the aptamers used were relatively short (<40 nt in length),[5,21−24] and very few studies have pertained to RNA aptamers.[25,26] Adaptability of the GO adsorption method toward longer aptamers would immensely enhance its utility. For example, RNA aptamers derived from riboswitches (systems that regulate gene expression in various organisms), are typically longer aptamers (>100 nt),[38] and have not yet been explored for graphene-based sensing. Many of these naturally occurring aptamers possess superior target-binding specificity and affinity,[39−42] and represent a class of aptamers that may be highly beneficial for sensor development.

Herein, we present a generalizable sensing strategy based on regulated GO adsorption that can accommodate RNA aptamers of various lengths. In our design, the 5′-end of an extended RNA aptamer is first hybridized to a complementary DNA strand that is modified with fluorophore (FDNA) (Figure 1,

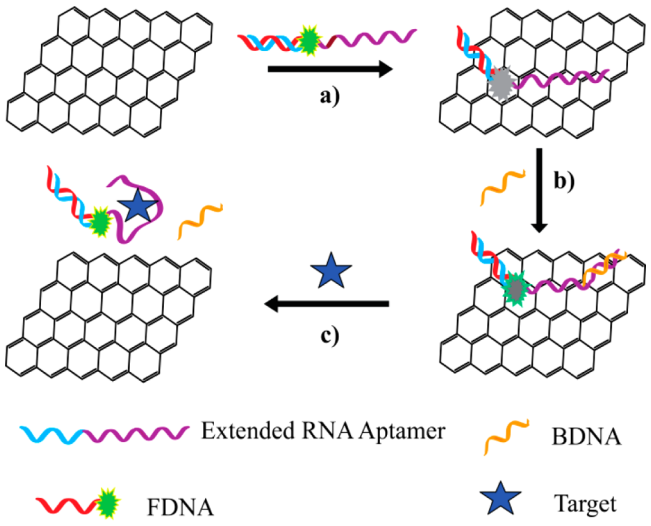

Figure 1. RNA aptamer sensors based on regulated graphene oxide (GO) adsorption. (reaction a) GO adsorption of duplex assembly between FDNA and Extended RNA Aptamer results in fluorescence quenching. (reaction b) Addition of BDNA leads to duplex formation with part of the aptamer, and weakening of GO adsorption to produce moderate fluorescence. (reaction c) The addition of target results in complete separation of the sensing system from GO, and high fluorescence is generated.

reaction a). Adsorption of this FDNA-RNA aptamer duplex to GO results in fluorescence quenching due to the close proximity of the fluorophore to GO. The addition of a complementary, "blocking" DNA strand (BDNA) that hybridizes to the 3′-end of the aptamer, weakens aptamer-GO interaction (Figure 1, reaction b), and enables higher fluorescent signal generation upon the addition of target, as the sensing system becomes completely separated from GO due to structure-switching (Figure 1, reaction c). Using this strategy, we have successfully engineered two sensors based on RNA aptamers that recognize theophylline and thiamine pyrophosphate (TPP), respectively.

2. EXPERIMENTAL SECTION

2.1. Materials. All DNA oligonucleotides were synthesized using automated DNA synthesis (Integrated DNA Technologies, Coralville, IA) following the standard phosphoramidite chemistry. The 5′-fluorescein in FDNA was introduced using 5′-fluorescein phosphoramidite. All DNA oligonucleotides were purified by 10% denaturing PAGE before use. FDNA was purified by HPLC. Graphene oxide was obtained from the Dalian University of Technology (Dalian, China) and was synthesized according to a modified Hummers method.[43] Unless otherwise noted, all other materials were purchased from Sigma (Oakville, Canada) and used without further purification.

2.2. Polymerase Chain Reaction. The theophylline DNA template with the sequence of 5′-GAATT CTAAT ACGAC TCACT ATAGG CCTGC CACGC TCCGA CGCTA TGGCG ATACC AGCCG AAAGG CCCTT GGCAG CGTC-3′ was amplified by PCR using 5′-GAATT CTAAT CGAC TCACT ATA-3′ and 5′-GACGC TGCCA AGG-3′ as forward and reverse primers. The TPP DNA template with the sequence of 5′-GAATT CTAAT ACGAC TCACT ATAGG CCTGC CACGC TCCGA CGCTA TCCAC TAGGG GTGCT TGTTG TGCTG AGAGA GGAAT AATCC TTAAC CCTTA TAACA CCTGA TCTAG GTAAT ACTAG CGAAG GGAAG TGG-3′ was obtained through T4 polynucleotide kinase (PNK)-mediated ligation of DNA template fragments. Ligation reaction was conducted according to manufacturer's protocol (Thermo Scientific, Canada). TPP template fragments with sequences of 5′-GAATT CTAAT ACGAC TCACT ATAGG CCTGC CACGC TCCGA CGCTA TCCAC TAGGG GTGCT TGTTG TGCTG AGAGA GGAAT AATCC TTAAC CCTTA TAACA CCTGA TCTAG GTAAT ACTAG CGAAG GGAAG TGG-3′ were ligated together using a ligation template sequence of 5′-CAGCA CAACA AGCAC CCCTA-3′. The final ligated TPP DNA template was then purified by 10% denaturing PAGE and amplified through PCR using 5′-GAATT CTAAT CGAC TCACT ATA-3′ (forward primer) and 5′-CCACT TCCCT TCGCT AGTAT-3′ (reverse primer). PCR was carried out in Tris·HCl (pH 9.0, 75 mM), $MgCl_2$ (2 mM), KCl (50 mM), $(NH_4)_2SO_4$ (20 mM), primers (0.5 μM of each), DNA template (3 nM), dNTPs (0.5 mM of each) and Taq DNA polymerase (5 units, Biotools, Madrid, Spain). Thermal cycling steps were 94 °C for 1 min, 18 cycles of 94 °C−45 °C−72 °C (30 s for each temperature), and finally 72 °C for 8 min.

2.3. RNA Transcription. The transcription reaction was conducted at 37 °C for 2.5 h in Tris-HCl (150 μL, 40 mM, pH 7.9), $MgCl_2$ (6 mM), dithiothreitol (DTT, 10 mM), NaCl (10 mM), spermidine (2 mM), PCR amplified DNA (25 pmol), NTPs (2.5 mM of each), RiboLock ribonuclease inhibitor (1.07 units/μL) and T7 RNA polymerase (1.33 units/μL, Thermo Scientific, Canada). The transcription mixture was then treated with DNase I (3 units, Thermo Scientific) in the presence of $CaCl_2$ (0.2 mM) at 37 °C for 15 min. The transcribed RNA was subsequently purified by 10% denaturing PAGE, and quantified by absorbance at 260 nm.

2.4. Fluorescence Measurements. For FDNA-RNA aptamer duplex assembly, a mixture of FDNA (200 nM) and RNA aptamer (200 nM), in a reaction buffer (50 μL total volume) of Tris-HCl (25 mM, pH 7.5) and $MgCl_2$ (10 mM) was first heated at 65 °C for 2 min, then cooled at room temperature for 10 min, and finally cooled at 4 °C for 10 min. GO (20 μL from 100 μg/mL stock) was then mixed into the FDNA-RNA aptamer mixture, and an aliquot (50 μL) was taken for analysis. All fluorescence readings were measured at 37 °C (unless stated otherwise) on Cary Eclipse spectrophotometer (Varian) with $\lambda_{ex}/\lambda_{em}$ of 490/520 nm. Aliquots of FDNA-RNA aptamer-GO were incubated at 37 °C for 30−60 min to reach stable background fluorescence and then the following was introduced: (i) BDNA only, (ii) target only or (iii) BDNA and then target/structural analogue. For

assays measuring fluorescence in real time, relative fluorescence (RF) was calculated by using F/F_0, where F_0 and F are the fluorescence intensity before and after the addition of BDNA/target, respectively. For assays measuring fluorescence spectra, fluorescence readings of test samples were recorded after 1 h incubation at 37 °C. For thermal denaturation profiles, each test sample was incubated at 20 °C for 5 min in the fluorimeter before the temperature was increased to 65 °C at a rate of 1 °C/min.

3. RESULTS AND DISCUSSION

3.1. Creation of an Aptamer Reporter for Theophylline. For the first demonstration, we chose the well-characterized theophylline RNA aptamer, a relatively short aptamer of 33 nt.[32,42] The DNA sequence that encodes both the FDNA-binding site and aptamer domain was chemically synthesized and amplified through polymerase chain reaction (PCR) using the necessary primers to produce a double-stranded DNA template. The PCR product was then used for in vitro transcription to generate the extended RNA aptamer. The sequence is presented in Figure 2A (aptamer domain in blue), along with relevant DNA sequences. The extended RNA aptamer was designed to form a duplex with an FDNA of 20 nt, which we have previously demonstrated to be a sufficient length for generating relatively low background and high target-induced signal enhancement.[32]

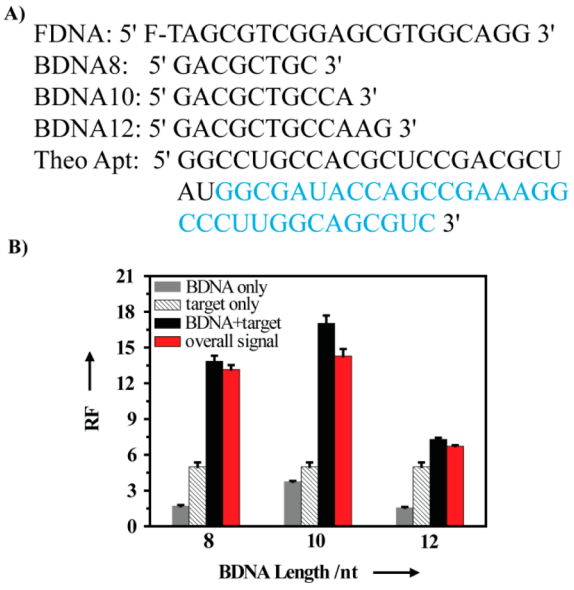

Figure 2. Creation of the theophylline reporter. (A) Sequences tested for the reporter (aptamer domain shown in blue). (B) Optimization of BDNA length (nucleotides, nt). FDNA-RNA Aptamer-GO was incubated for 30 min, then BDNA (gray, 400 nM), theophylline target (striped, 800 μM), or a combination of BDNA+target (black) was added. Relative fluorescence (RF) was plotted after 1 h. RF = F_t/F_0, fluorescence intensity at time t and 0. Calculation of overall signal enhancement (shown in red) = [BDNA+target]-BDNA. The data are an average of two independent experiments.

In our preliminary analysis, we optimized the experimental conditions necessary for target detection using the classic method of GO adsorption. We systematically tested each relevant factor by assessing the theophylline-sensing ability of the FDNA-RNA aptamer duplex adsorbed to GO. By assessing concentrations of divalent metal ion (see Figure S1A in the Supporting Information), FDNA (see Figure S1B in the Supporting Information) and GO (see Figure S1C in the Supporting Information), as well as temperature (see Figure S1D, E in the Supporting Information), we determined the optimal conditions to minimize background fluorescence, and generate the highest fluorescent signal enhancement possible using this design. The maximum fold enhancement was found to be ~5-fold.

To further enhance signaling ability, we designed various lengths of BDNA (8−12 nt) to hybridize to the 3′-end of the theophylline aptamer (Figure 2A). For all BDNA lengths, we found that the addition of theophylline and BDNA together significantly enhanced fluorescent signal, even after subtraction of BDNA background (black and red data sets respectively, Figure 2B), as compared to the addition of BDNA or target only (gray and striped data sets respectively, Figure 2B). Particularly, BDNA length of 10 nt (BDNA10) generated the highest signal enhancement and was chosen for further analysis (Figure 2B).

To investigate the mechanism of BDNA for signal enhancement, we tested the effect of various BDNA10 concentrations on the FDNA-RNA aptamer-GO system. In samples treated with BDNA10 alone, we discovered that increasing BDNA10 concentration expectedly led to increasing background signal, which signifies increasing FDNA-RNA aptamer dissociation from GO (gray data set, Figure 3A). The ability of BDNA10 to weaken FDNA-RNA aptamer interaction with GO was also confirmed in our thermal denaturation analysis (Figure 3B). In this assay, the control sample of FDNA-RNA aptamer-GO produced the expected low fluorescence at all temperatures signifying absorption of FDNA-RNA aptamer to GO (black data set, Figure 3B). However, the addition of BDNA10 to FDNA-RNA aptamer-GO resulted in relatively high fluorescence at lower testing temperatures, and a gradual decrease in fluorescence with increasing temperature. These results confirm that when the temperature is lower than the melting temperature of BDNA10 (T_M = 41 °C, predicted by IDT

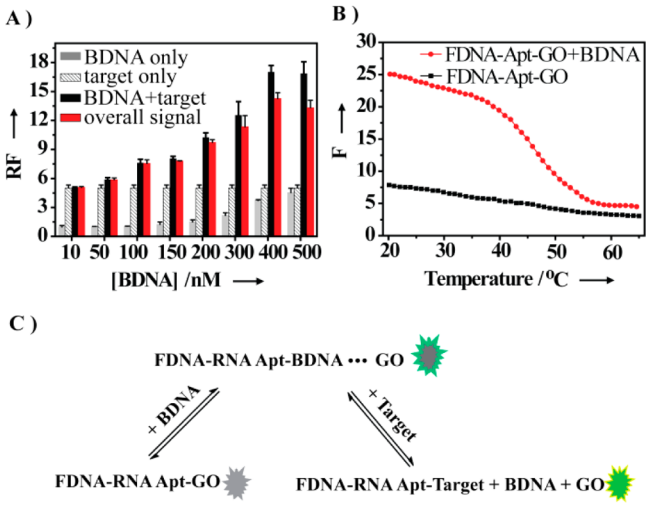

Figure 3. BDNA mechanism for signal enhancement. (A) Testing the effect of increasing BDNA concentration. FDNA-RNA Aptamer-GO was incubated for 30 min, then BDNA (gray, 10−500 nM), theophylline target (striped, 800 μM), or a combination of BDNA +target (black) was added. RF was plotted after 1 h. Overall signal enhancement shown in red. (B) Thermal denaturation profiles of FDNA-RNA Aptamer-GO system with the addition of BDNA (red), or without BDNA (black). All data are an average of two independent experiments. (C) Summary of sensing scheme.

Oligo Analyzer), BDNA10 can hybridize to FDNA-RNA aptamer and weaken GO adsorption to generate moderate fluorescence (red data set, Figure 3B). In contrast, at higher temperatures, BDNA10 remains unhybridized and FDNA-RNA aptamer can strongly absorb to GO for fluorescence quenching (red data set, Figure 3B). Notably, a small gradual decrease in fluorescence was found from low to high temperatures for both samples. This may be due to the well established effect of temperature on fluorophore emission,[44,45] as well as GO solubility.[46,47] In further testing, we found that the addition of a fixed concentration of theophylline along with increasing BDNA10 concentration (black data set, Figure 3A) resulted in increased overall signal enhancement (red data set, Figure 3A), as compared to the addition of either theophylline or BDNA10 alone (striped data set, and gray data set, Figure 3A). The optimal BDNA10 concentration was determined to be 400 nM since the highest signal enhancement was generated: ~17-fold raw fluorescent value before subtraction of signal produced by BDNA10 (black data set, Figure 3A), ~14-fold finalized value after subtraction of BDNA10 signal (red data set, Figure 3A), which are respectively 12- and 9-fold higher than the addition of theophylline alone (striped data set, Figure 3A). Taken together, the optimal setting requires 200 nM FDNA and 200 nM RNA aptamer to facilitate the formation of the FDNA-RNA aptamer duplex. A relative excess of GO (2 μg) is needed to quench FDNA and minimize background fluorescence. Additionally, a relative excess of BDNA10 (400 nM) is also needed to fully displace the sensing system from GO for optimal fluorescence signal generation (higher concentrations of BDNA10 do not generate any further increase in signal) (black and red data sets, Figure 3A).

Overall, the mechanism of the sensing system is summarized in Figure 3C, whereby FDNA-RNA aptamer duplex is initially absorbed onto GO to produce low fluorescence (FDNA-RNA Apt-GO). The addition of BDNA forms a duplex with the 3′ end of the aptamer and weakens aptamer interaction with GO to generate moderate fluorescence (FDNA-RNA Apt-BDNA···GO). The addition of target in the final step results in the formation of FDNA-RNA Apt-Target complex, and dissociation of BDNA. Complete separation of the sensing system from GO leads to high fluorescence signal generation. In combination, the addition of target and BDNA together can shift the equilibrium to form FDNA-RNA Apt-Target complex better than either target or BDNA alone.

3.2. Sensing Capability of Theophylline Reporter. The FDNA-aptamer-GO-BDNA10 system was found to be highly specific for theophylline detection. The addition of BDNA10 along with structural derivatives theobromine or caffeine generated relatively low fluorescent signals, which were comparable to the sample treated with BDNA10 alone (Figure 4A). Similarly, mutation of aptamer nucleotides known to be critical for theophylline recognition abolished binding activity, as a low fluorescent signal was produced (Figure 4A and sequence found in Figure S2A in the Supporting Information). To determine the sensitivity of the system, fluorescent signal was measured at various theophylline concentrations. The detection limit was found to be 0.5 μM, and the dynamic detection window was between 0.5−2000 μM (Figure 4B). The relative fluorescence observed at 1 h versus theophylline concentration is provided in Figure 4C, D.

3.3. Creation of an Aptamer Reporter for TPP. To demonstrate that our novel sensing strategy is generalizable and can accommodate longer RNA aptamers, we chose the TPP

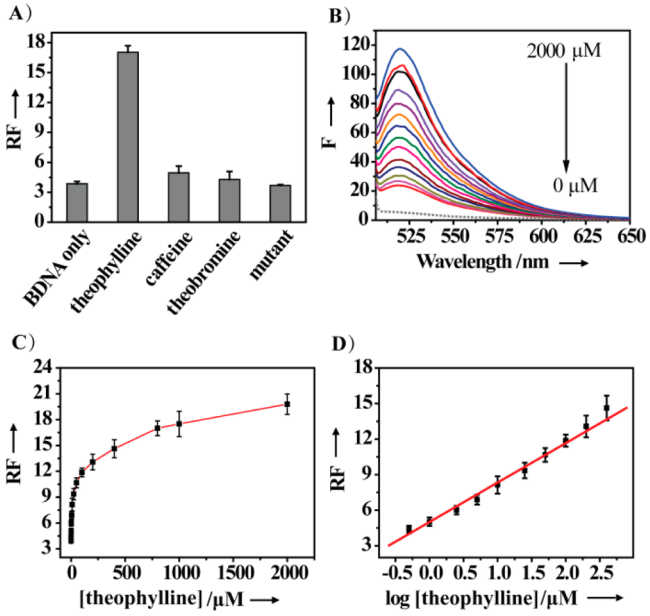

Figure 4. Sensing capability of the theophylline reporter. (A) Specificity test. FDNA-RNA Aptamer-GO was incubated for 30 min, then BDNA (400 nM) was added, and finally theophylline (800 μM), caffeine (800 μM), theobromine (800 μM), or no addition (BDNA only) was introduced. Mutant aptamer was tested with theophylline. RF was plotted after 1 h. (B) Fluorescence spectra of FDNA-RNA Aptamer-GO (dotted line), and after the addition of BDNA10 (400 nM) along with theophylline (0, 0.5, 1, 2.5, 5, 10, 25, 50, 100, 200, 400, 800, 1000, and 2000 μM). (C) Signal response of the reporter to theophylline concentration. (D) Signal response to logarithm of theophylline concentration. The data are an average of two independent experiments.

aptamer as the second example. The TPP aptamer is 87 nt in length, and derived from a well-characterized riboswitch that is found in diverse organisms.[32,48] The design of the TPP reporter was mostly based on our findings from the theophylline reporter and used the same 20-nt FDNA sequence (all sequences presented in Figure 5A, aptamer domain in blue), as well as the optimized conditions for sensing (see Figure S1 in the Supporting Information). The only difference was the BDNA sequence required. By testing various BDNA lengths (10−15 nt), the BDNA length of 13 nt (BDNA13) was found to be optimal since the highest overall signal enhancement of ~3-fold was produced (red data set, Figure 5B), which is 2× higher than the enhancement from TPP addition alone (striped data set, Figure 5B).

3.4. Sensing Capability of TPP Reporter. The TPP reporter could also detect TPP specifically, as the addition of structural derivatives thiamine monophosphate (TMP), thiamine, or oxythiamine generated low fluorescent levels, which were comparable to the sample treated with BDNA13 only (Figure 6A). Likewise, mutation of aptamer nucleotides that are known to be critical for TPP recognition, also abolished target binding as low fluorescence was generated (Figure 6A and sequence found in Figure S2B in the Supporting Information). The detection limit was determined to be 0.01 μM, and the dynamic detection window was between 0.01 and 100 μM (Figure 6B). The relative fluorescence observed at 1 h versus TPP concentration is found in Figure 6 (panels C and D).

3.5. Assessment of Regulated GO Adsorption for Sensor Development. Using this strategy, sensors were

A)

FDNA: 5' F-TAGCGTCGGAGCGTGGCAGG 3'
BDNA10: 5' CCACTTCCCT 3'
BDNA12: 5' CCACTTCCCTTC 3'
BDNA13: 5' CCACTTCCCTTCG 3'
BDNA15: 5' CCACTTCCCTTCGCT 3'
TPP Apt: 5' GGCCUGCCACGCUCCGACGCUA
UCCACUAGGGGUGCUUGUUGUG
CUGAGAGAGGAAUAAUCCUUAA
CCCUUAUAACACCUGAUCUAGG
UAAUACUAGCGAAGGGAAGUGG 3'

B)

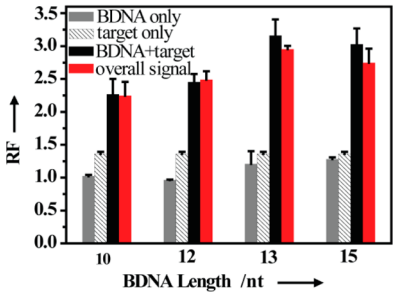

Figure 5. Creation of the TPP reporter. (A) Sequences tested for the reporter (aptamer domain shown in blue). (B) Optimization of BDNA length (nt). FDNA-RNA Aptamer-GO was incubated for 1 h, then BDNA (gray, 400 nM), TPP target (striped, 100 μM), or a combination of BDNA+target (black) was added. RF was plotted after 1 h. Overall signal enhancement is shown in red. The data are an average of two independent experiments.

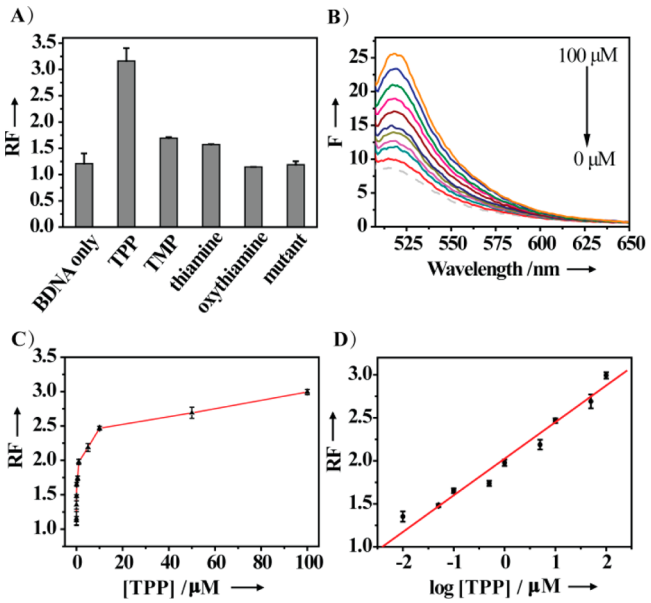

Figure 6. Sensing capability of the TPP reporter. (A) Specificity test. FDNA-RNA Aptamer-GO was incubated for 1 h, then BDNA13 (400 nM) was added, and finally TPP (100 μM), TMP (100 μM), thiamine (100 μM), oxythiamine (100 μM), or no addition (BDNA only) was introduced. Mutant aptamer was tested with TPP. RF was plotted after 1 h. (B) Fluorescence spectra of FDNA-RNA Aptamer-GO (dotted line), and after the addition of BDNA13 (400 nM) along with TPP (0, 0.01, 0.05, 0.1, 0.5, 1, 5, 10, 50, and 100 μM). (C) Signal response of the reporter to TPP concentration. (D) Signal response to logarithm of TPP concentration. The data are an average of two independent experiments.

created for both the relatively shorter theophylline aptamer, as well as the relatively longer TPP aptamer. Both reporters retained a detection limit and binding specificity that are characteristic of the original aptamers,[42,48] and these results are consistent with previous structure-switching studies.[32,49] Importantly, given that this new strategy of regulated GO adsorption maximizes fluorescent signal generation in contrast to the classic GO adsorption method, relatively lower detection limits are obtainable. For instance, in the presence of BDNA and target together, the theophylline reporter generated a detection limit of 0.5 μM (Figure 4B), which is 20-fold lower than in the absence of BDNA using the classic GO adsorption method (detection limit ~10 μM) (red data set, see Figure S3A in the Supporting Information). Notably in contrast, at the concentration of 10 μM theophylline, the presence of BDNA and target together was able to generate over 6-fold signal enhancement (blue data set, see Figure S3A in the Supporting Information). Indeed, even better detection limits may be achieved by coupling our new sensing strategy with a signal amplification method to generate higher fluorescence per aptamer-target binding interaction, or to facilitate a greater overall number of aptamer-target binding interactions (and in effect lower background fluorescence). Several of these amplification methods have already been demonstrated for graphene-based sensing.[22,50−55] Furthermore, integration of our new sensing strategy with more sensitive signal transduction methods such as chemiluminescence may further lower the limit of detection as previous studies have shown.[56,57]

Another advantage of the regulated GO adsorption method is that it can speed up signal response time. For example, when using the classic GO adsorption method (absence of BDNA) for the theophylline reporter, ~15 min were required to reach the maximum ~4.5-fold signal enhancement upon the addition of high theophylline concentration (red data set, Figure S3B in the Supporting Information). However, in the presence of BDNA and theophylline together, this level of signal was reached within 1 min (blue data set, Figure S3B in the Supporting Information).

For both theophylline and TPP reporters, BDNA incorporation substantially increased overall signal enhancement compared to the addition of target alone. The theophylline reporter produced an overall 14-fold signal enhancement, which is 9-fold greater than the addition of theophylline alone (Figure 3A). Similarly, the TPP reporter produced a 3-fold signal enhancement, 2× greater than the addition of TPP alone (Figure 5B). Notably, overall BDNA-mediated signal enhancement for the theophylline reporter is higher than for the TPP reporter. We speculate that FDNA-RNA aptamer adsorption to GO is stronger for the TPP aptamer than for the theophylline aptamer due to longer sequence length.[34−36] As a result, the overall signal enhancement for the TPP reporter is reduced possibly because more copies of FDNA-RNA aptamer are unable to switch off from GO, even after the addition of BDNA. To obtain higher signal enhancement particularly when using longer aptamers, implementation of fluorescent signal amplification strategies may be beneficial (as described above).

4. CONCLUSIONS

In summary, we have demonstrated a generalizable strategy to create fluorescent sensors based on regulated GO adsorption that can accommodate RNA aptamers of various lengths. The sensing strategy makes use of the fluorescence quenching property of GO when it comes in contact with an FDNA-

labeled RNA aptamer. The introduction of a BDNA sequence that forms a duplex with the 3′ end of the aptamer provides a novel way to weaken aptamer-GO interaction. In effect, the addition of BDNA and target together can facilitate separation of the sensing system from GO and provide greater signal enhancement, compared to the existing, classical method of GO adsorption.

Future application of regulated GO adsorption may lead to further exploration of less characterized aptamers. Furthermore, adaptation of this strategy toward previously reported studies using classic GO adsorption, may enhance the generality of these methods, which have been implemented for important applications such as the detection of multiple targets[25,58] and live cell analysis.[5]

■ ASSOCIATED CONTENT

Ⓢ Supporting Information

Data to optimize RNA aptamer sensor using classic GO adsorption method, sequences of theophylline and TPP mutant aptamers, data to compare sensing capability of regulated GO adsorption and classic GO adsorption methods.This material is available free of charge via the Internet at http://pubs.acs.org.

■ AUTHOR INFORMATION

Corresponding Author

*E-mail: liying@mcmaster.ca.

Present Address

[§]J.S. is currently at College of Chemistry and Environmental Engineering and Institute of Applied Chemistry, Shanxi Datong University, Datong, Shanxi, 037009, China

Author Contributions

[⊥]Authors J.S. and P.S.L. contributed equally. The manuscript was written through contributions of all authors. All authors have given approval to the final version of the manuscript.

Notes

The authors declare no competing financial interest.

■ ACKNOWLEDGMENTS

This work was supported by research grants from Natural Sciences and Engineering Research Council of Canada (NSERC) via a Discovery grant to Y.L. and a postgraduate scholarship to P.S.L., Shanxi Province Hundred Talent Project Support, and the Canadian Food Inspection Agency (CFIA) via a studentship to P.S.L.

■ REFERENCES

(1) Novoselov, K. S.; Geim, A. K.; Morozov, S. V.; Jiang, D.; Zhang, Y.; Dubonos, S. V.; Grigorieva, I. V.; Firsov, A. A. Electric Field Effect in Atomically Thin Carbon Films. *Science* **2004**, *306*, 666−669.

(2) Sharma, P. S.; D'Souza, F.; Kutner, W. Graphene and Graphene Oxide Materials for Chemo- and Biosensing of Chemical and Biochemical Hazards. *Top. Curr. Chem.* **2013**.

(3) Geim, A. K. Graphene: Status and Prospects. *Science* **2009**, *324*, 1530−1534.

(4) Zeng, Q. O.; Cheng, J. S.; Tang, L. H.; Liu, X. F.; Liu, Y. Z.; Li, J. H.; Jiang, J. H. Self-assembled Graphene-enzyme Hierarchical Nanostructures for Electrochemical Biosensing. *Adv. Funct. Mater.* **2010**, *20*, 3366−3372.

(5) Wang, Y.; Li, Z.; Hu, D.; Lin, C. T.; Li, J.; Lin, Y. Aptamer/graphene Oxide Nanocomplex for In Situ Molecular Probing in Living Cells. *J. Am. Chem. Soc.* **2010**, *132*, 9274−9276.

(6) Wang, Y.; Lu, J.; Tang, L.; Chang, H.; Li, J. Graphene Oxide Amplified Electrogenerated Chemiluminescence of Quantum Dots and Its Selective Sensing for Glutathione from Thiol-containing Compounds. *Anal. Chem.* **2009**, *81*, 9710−9715.

(7) Wang, Y.; Li, Y. M.; Tang, L. H.; Lu, J.; Li, J. H. Application of Graphene-modified Electrode for Selective Detection of Dopamine. *Electrochem. Commun.* **2009**, *11*, 889−892.

(8) Shen, X.; Jiang, L.; Ji, Z.; Wu, J.; Zhou, H.; Zhu, G. Stable Aqueous Dispersions of Graphene Prepared with Hexamethylenetetramine as a Reductant. *J. Colloid Interface Sci.* **2011**, *354*, 493−497.

(9) Hummers, W. S.; Offeman, R. E. Preparation of Graphitic Oxide. *J. Am. Chem. Soc.* **1958**, *80*, 1339−1339.

(10) Staudenmaier, L. Verfahren zur Darstellung der Graphitsäure. *Ber. Dtsch. Chem. Ges.* **1898**, *31*, 1481−1487.

(11) Chandra, S.; Sahu, S.; Pramanik, P. A Novel Synthesis of Graphene by Dichromate Oxidation. *Mater. Sci. Eng. B* **2010**, *167*, 133−136.

(12) Kumar, A.; Voevodin, A. A.; Paul, R.; Altfeder, I.; Zemlyanov, D.; Zakharov, D. N.; Fisher, T. S. Nitrogen-doped Graphene by Microwave Plasma Chemical Vapor Deposition. *Thin Solid Films* **2013**, *528*, 269−273.

(13) Ramachandran, R.; Mani, V.; Chen, S. M.; Saraswathi, R.; Lou, B. S. Recent Trends in Graphene Based Electrode Materials for Energy Storage Devices and Sensors Applications. *Int. J. Electrochem. Sci.* **2013**, *8*, 11680−11694.

(14) Wei, D.; Kivioja, J. Graphene for Energy Solutions and Its Industrialization. *Nanoscale* **2013**, *5*, 10108−10126.

(15) *The World Market for Graphene to 2017*; Future Markets Inc., 2011.

(16) Zhang, L.; Lu, Z.; Zhao, Q.; Huang, J.; Shen, H.; Zhang, Z. Enhanced Chemotherapy Efficacy by Sequential Delivery of siRNA and Anticancer Drugs Using PEI-grafted Graphene Oxide. *Small* **2011**, *7*, 460−464.

(17) Liu, Z.; Robinson, J. T.; Sun, X.; Dai, H. PEGylated Nanographene Oxide for Delivery of Water-insoluble Cancer Drugs. *J. Am. Chem. Soc.* **2008**, *130*, 10876−10877.

(18) Sun, X.; Liu, Z.; Welsher, K.; Robinson, J. T.; Goodwin, A.; Zaric, S.; Dai, H. Nano-graphene Oxide for Cellular Imaging and Drug Delivery. *Nano Res.* **2008**, *1*, 203−212.

(19) Yang, K.; Zhang, S.; Zhang, G.; Sun, X.; Lee, S. T.; Liu, Z. Graphene in Mice: Ultrahigh In Vivo Tumor Uptake and Efficient Photothermal Therapy. *Nano Lett.* **2010**, *10*, 3318−3323.

(20) Lu, C. H.; Yang, H. H.; Zhu, C. L.; Chen, X.; Chen, G. N. A Graphene Platform for Sensing Biomolecules. *Angew. Chem., Int. Ed. Engl.* **2009**, *48*, 4785−4787.

(21) Chang, H.; Tang, L.; Wang, Y.; Jiang, J.; Li, J. Graphene Fluorescence Resonance Energy Transfer Aptasensor for the Thrombin Detection. *Anal. Chem.* **2010**, *82*, 2341−2346.

(22) Pu, Y.; Zhu, Z.; Han, D.; Liu, H.; Liu, J.; Liao, J.; Zhang, K.; Tan, W. Insulin-binding Aptamer-conjugated Graphene Oxide for Insulin Detection. *Analyst* **2011**, *136*, 4138−4140.

(23) He, Y.; Wang, Z. G.; Tang, H. W.; Pang, D. W. Low Background Signal Platform for the Detection of ATP: When a Molecular Aptamer Beacon Meets Graphene Oxide. *Biosens. Bioelectron.* **2011**, *29*, 76−81.

(24) Sheng, L.; Ren, J.; Miao, Y.; Wang, J.; Wang, E. PVP-coated Graphene Oxide for Selective Determination of Ochratoxin A via Quenching Fluorescence of Free Aptamer. *Biosens. Bioelectron.* **2011**, *26*, 3494−3499.

(25) Wang, Y.; Li, Z.; Weber, T. J.; Hu, D.; Lin, C. T.; Li, J.; Lin, Y. In Situ Live Cell Sensing of Multiple Nucleotides Exploiting DNA/RNA Aptamers and Graphene Oxide Nanosheets. *Anal. Chem.* **2013**, *85*, 6775−6782.

(26) Cui, L.; Chen, Z.; Zhu, Z.; Lin, X.; Chen, X.; Yang, C. J. Stabilization of ssRNA on Graphene Oxide Surface: an Effective Way to Design Highly Robust RNA Probes. *Anal. Chem.* **2013**, *85*, 2269−2275.

(27) Ellington, A. D.; Szostak, J. W. In Vitro Selection of RNA Molecules that Bind Specific Ligands. *Nature* **1990**, *346*, 818−822.

(28) Tuerk, C.; Gold, L. Systematic Evolution of Ligands by Exponential Enrichment: RNA Ligands to Bacteriophage T4 DNA Polymerase. *Science* **1990**, *249*, 505−510.

(29) Nutiu, R.; Li, Y. Structure-switching Signaling Aptamers: Transducing Molecular Recognition into Fluorescence Signaling. *Chemistry* **2004**, *10*, 1868−1876.
(30) Nutiu, R.; Li, Y. Aptamers with Fluorescence-signaling Properties. *Methods* **2005**, *37*, 16−25.
(31) Nutiu, R.; Li, Y. Structure-switching Signaling Aptamers. *J. Am. Chem. Soc.* **2003**, *125*, 4771−4778.
(32) Lau, P. S.; Coombes, B. K.; Li, Y. A General Approach to the Construction of Structure-switching Reporters from RNA Aptamers. *Angew. Chem., Int. Ed.*. **2010**, *49*, 7938−7942.
(33) Liu, Y.; Dong, X.; Chen, P. Biological and Chemical Sensors Based on Graphene Materials. *Chem. Soc. Rev.* **2012**, *41*, 2283−2307.
(34) Manohar, S.; Mantz, A. R.; Bancroft, K. E.; Hui, C. Y.; Jagota, A.; Vezenov, D. V. Peeling Single-stranded DNA from Graphite Surface to Determine Oligonucleotide Binding Energy by Force Spectroscopy. *Nano Lett.* **2008**, *8*, 4365−4372.
(35) Sowerby, S. J.; Cohn, C. A.; Heckl, W. M.; Holm, N. G. Differential Adsorption of Nucleic Acid Bases: Relevance to the Origin of Life. *Proc. Natl. Acad. Sci. U.S.A.* **2001**, *98*, 820−822.
(36) Sowerby, S. J.; Morth, C. M.; Holm, N. G. Effect of Temperature on the Adsorption of Adenine. *Astrobiology* **2001**, *1*, 481−487.
(37) Liu, B.; Sun, Z.; Zhang, X.; Liu, J. Mechanisms of DNA Sensing on Graphene Oxide. *Anal. Chem.* **2013**, *85*, 7987−7993.
(38) Breaker, R. R. In *The RNA World*; Gesteland, R. F., Cech, T. R., Atkins, J. F., Eds.; Cold Spring Harbor Laboratory Press: Cold Spring Harbor, NY, 2006; Chapter: Riboswitches and the RNA World, pp 89−107.
(39) Navani, N. K.; Li, Y. Nucleic Acid Aptamers and Enzymes as Sensors. *Curr. Opin. Chem. Biol.* **2006**, *10*, 272−281.
(40) Famulok, M.; Mayer, G. Aptamer Modules as Sensors and Detectors. *Acc. Chem. Res.* **2011**, *44*, 1349−1358.
(41) Wang, J. X.; Lee, E. R.; Morales, D. R.; Lim, J.; Breaker, R. R. Riboswitches that Sense S-adenosylhomocysteine and Activate Genes Involved in Coenzyme Recycling. *Mol. Cell* **2008**, *29*, 691−702.
(42) Jenison, R. D.; Gill, S. C.; Pardi, A.; Polisky, B. High-resolution Molecular Discrimination by RNA. *Science* **1994**, *263*, 1425−1429.
(43) Liu, M.; Zhang, Q.; Zhao, H.; Chen, S.; Yu, H.; Zhang, Y.; Quan, X. Controllable Oxidative DNA Cleavage-dependent Regulation of Graphene/DNA Interaction. *Chem. Commun.* **2011**, *47*, 4084−4086.
(44) Estrada-Perez, C. E.; Hassan, Y. A.; Tan, S. C. Experimental Characterization of Temperature Sensitive Dyes for Laser Induced Fluorescence Thermometry. *Rev. Sci. Instrum.* **2011**, *82*.
(45) Guan, X. L.; Liu, X. Y.; Su, Z. X.; Liu, P. The Preparation and Photophysical Behaviors of Temperature/pH-sensitive Polymer Materials Bearing Fluorescein. *React. Funct. Polym.* **2006**, *66*, 1227−1239.
(46) Zhou, Y.; Bao, Q. L.; Tang, L. A. L.; Zhong, Y. L.; Loh, K. P. Hydrothermal Dehydration for the "Green" Reduction of Exfoliated Graphene Oxide to Graphene and Demonstration of Tunable Optical Limiting Properties. *Chem. Mater.* **2009**, *21*, 2950−2956.
(47) Zhu, Y. W.; Stoller, M. D.; Cai, W. W.; Velamakanni, A.; Piner, R. D.; Chen, D.; Ruoff, R. S. Exfoliation of Graphite Oxide in Propylene Carbonate and Thermal Reduction of the Resulting Graphene Oxide Platelets. *ACS Nano* **2010**, *4*, 1227−1233.
(48) Welz, R.; Breaker, R. R. Ligand Binding and Gene Control Characteristics of Tandem Riboswitches in Bacillus anthracis. *RNA* **2007**, *13*, 573−582.
(49) Lau, P. S.; Lai, C. K.; Li, Y. Quality Control Certification of RNA Aptamer-based Detection. *Chembiochem* **2013**, *14*, 987−992.
(50) Chen, C.; Zhao, J.; Jiang, J.; Yu, R. A Novel Exonuclease III-aided Amplification Assay for Lysozyme Based on Graphene Oxide Platform. *Talanta* **2012**, *101*, 357−361.
(51) Hu, P.; Zhu, C.; Jin, L.; Dong, S. An Ultrasensitive Fluorescent Aptasensor for Adenosine Detection Based on Exonuclease III Assisted Signal Amplification. *Biosens. Bioelectron.* **2012**, *34*, 83−87.
(52) Zhao, X. H.; Ma, Q. J.; Wu, X. X.; Zhu, X. Graphene Oxide-based Biosensor for Sensitive Fluorescence Detection of DNA Based on Exonuclease III-aided Signal Amplification. *Anal. Chim. Acta* **2012**, *727*, 67−70.
(53) Hu, K.; Liu, J.; Chen, J.; Huang, Y.; Zhao, S.; Tian, J.; Zhang, G. An Amplified Graphene Oxide-based Fluorescence Aptasensor Based on Target-triggered Aptamer Hairpin Switch and Strand-Displacement Polymerization Recycling for Bioassays. *Biosens. Bioelectron.* **2013**, *42*, 598−602.
(54) Liu, J.; Wang, C.; Jiang, Y.; Hu, Y.; Li, J.; Yang, S.; Li, Y.; Yang, R.; Tan, W.; Huang, C. Z. Graphene Signal Amplification for Sensitive and Real-time Fluorescence Anisotropy Detection of Small Molecules. *Anal. Chem.* **2013**, *85*, 1424−1430.
(55) Li, X.; Song, J.; Wang, Y.; Cheng, T. Cyclically Amplified Fluorescent Detection of Theophylline and Thiamine Pyrophosphate by Coupling Self-cleaving RNA Ribozyme with Endonuclease. *Anal. Chim. Acta* **2013**, *797*, 95−101.
(56) He, Y.; Huang, G.; Cui, H. Quenching the Chemiluminescence of Acridinium Ester by Graphene Oxide for Label-free and Homogeneous DNA Detection. *ACS Appl. Mater. Interfaces* **2013**, *5*, 11336−11340.
(57) Chen, C.; Li, B. Graphene Oxide-based Homogenous Biosensing Platform for Ultrasensitive DNA Detection Based on Chemiluminescence Resonance Energy Transfer and Exonuclease III-assisted Target Recycling Amplification. *J. Mater. Chem. B* **2013**, *1*, 2476−2481.
(58) Wang, L.; Zhu, J.; Han, L.; Jin, L.; Zhu, C.; Wang, E.; Dong, S. Graphene-based Aptamer Logic Gates and Their Application to Multiplex Detection. *ACS Nano* **2012**, *6*, 6659−6666.